Journal of King Saud University – Computer and Information Sciences (2015) 27, 140–146

King Saud University
Journal of King Saud University – Computer and Information Sciences
www.ksu.edu.sa
www.sciencedirect.com

Admissible curvature continuous areas for fair curves using G^2 Hermite PH quintic polynomial

Zulfiqar Habib [a,*], **Ghulam Rasool** [a], **Manabu Sakai** [b]

[a] *Department of Computer Science, COMSATS Institute of Information Technology, Ali Akbar Road, Lahore, Pakistan*
[b] *Department of Mathematics & Computer Science, Kagoshima University, Kagoshima, Japan*

Received 26 August 2013; revised 6 December 2013; accepted 13 March 2014
Available online 27 March 2015

KEYWORDS
Motion planning;
Pythagorean hodograph (PH);
Quintic polynomial;
G^2 Hermite;
Monotone;
Curvature

Abstract In this paper we derive admissible curvature continuous areas for monotonically increasing curvature continuous smooth curve by using a single Pythagorean hodograph (PH) quintic polynomial of G^2 contact matching Hermite end conditions. Curves with monotonically increasing or decreasing curvatures are considered highly smooth (fair) and are very useful in geometric design. Making the design by using smooth curves is a fascinating problem of computing with significant physical and esthetic applications especially in high speed transportation and robotics. First we derive sufficient conditions for curvature continuity on a single PH quintic polynomial with given Hermite end conditions then we find the admissible area for the smooth curve with respect to the curvatures at its endpoints.

1. Introduction

It is often desirable to have curvature continuous smooth curves of G^2 contact matching Hermite end conditions, i.e., spiral segments, in geometric design of curves and surfaces. The purpose may be aesthetic applications in information technology (Burchard et al., 1993), practical applications such as in robotics, GIS, CAD systems, animations, environmental design, collision avoidance, animations, satellite path planning, highway/railway design, geometric modeling, surface reconstruction, and other disciplines (Farin, 2002; Hanmandlu et al., 2003; Sarfraz, 2004; Habib, 2010; Habib and Sakai, 2012). Curvature continuous curves are considered highly smooth and fair, i.e., these curves are free from superfluous inflection points, curvature extrema, loops, and cusps (Habib, 2010; Deng and Ma, 2012).

Cubic splines in parametric form are usually used in computer aided geometric design and manufacturing processes due to their numerical and geometric features. However a cubic curve is not always helpful and suitable because its arc-length is the integral part of the square root of a polynomial of its parameter and its offset is neither polynomial, nor a rational algebraic function of its parameter (Ait-Haddou, 1995).

Farouki and Sakkalis (1990) introduced Pythagorean hodograph (PH) curves which do not suffer from the above mentioned unwanted features of cubic polynomials and are

* Corresponding author.
E-mail addresses: drzhabib@ciitlahore.edu.pk (Z. Habib), grasool@ciitlahore.edu.pk (G. Rasool), msakai@sci.kagoshima-u.ac.jp (M. Sakai).
Peer review under responsibility of King Saud University.

Production and hosting by Elsevier

http://dx.doi.org/10.1016/j.jksuci.2014.03.016
1319-1578

very useful in curve fairing (Habib and Sakai, 2013). The lowest degree PH curves having reasonable flexibility for geometric design are, in general, the polynomials of quintic order (Farouki and Neff, 1995; Habib and Sakai, 2008). However, both cubic and quintic polynomials may have more curvature extrema than required (Habib, 2010). Farin (2002) pointed out that "curvature extrema of a fair curve should only occur where it is explicitly required by the designer". It can be achieved while the design is prepared by imposing curvature continuous conditions. The clothoid spiral is a non-polynomial which has been applied in highway designs for many years (Hartman, 1957). Unfortunately, it is not convenient to include clothoid in computer aided design systems due to its features that it is neither a polynomial nor a rational curve. Previously, fair curves had been formed using two curve segments, in particular, two clothoid spiral segments (Meek and Walton, 1989), two cubic spiral segments, and two PH quintic spiral segments (Walton and Meek, 2007). It is disadvantageous for the designers to use two segments as compared to a single one because they have to deal with more entities.

Spiral segments of G^2 contact have been considered for transition between (i) straight line and circle, (ii) two circles with a broken back C-shape, (iii) two circles with an S-shape, (iv) two straight lines (v) two circles where one circle lies inside the other with a C-shape, known as the fifth case (Walton et al., 2003; Habib, 2010).

1.1. Problem statement

The fifth case used in highway and railway design has not been solved completely by this time. Numerical treatment of the case would imply that it does not always seem to have a solution due to the absence of necessary conditions (Sarpono et al., 2009; Habib, 2010). Maximum possible admissible curvature continuous areas (CCA) where the designer can find spiral segments are explored by using the rational cubic polynomial in Habib and Sakai (2010). Due to the importance of PH quintic polynomial in geometric design, our focus in this paper is to develop a simple algorithm for maximum possible admissible CCA by using a single PH quintic function (Habib and Sakai, 2010).

1.2. Related works

State-of-the-art approaches discussed the significance of using smooth curves in the design process. Sarpono et al. (2009) considered the single curve of G^2 contact but it may have unnecessary internal curvature extrema. The curvature continuous form of G^2 contact is then derived in Habib and Sakai (2007b, 2008). However, it is not matching exactly Hermite end conditions, i.e., endpoints and tangents at these endpoints are not fixed in these methods.

Dietz and Piper (2004) proposed a method by using numerical techniques to study curvature continuous cubic polynomial matching G^2 Hermite data and derived tables for adjustment of curvatures at the endpoints. Their work was continued and extended in Dietz et al. (2008), Habib and Sakai (2010, 2011) by using cubic and rational cubic functions. Free parameters were used to find more CCA but these were at the cost of a lengthy and dreary procedure of finding a cubic or rational cubic curvature continuous curves. Due to the limitations of cubic polynomial as mentioned above and successful use of higher order polynomials in design applications (Farouki and Sakkalis, 1990; Farouki and Neff, 1995; Habib and Sakai, 2007b,a, 2008; Walton and Meek, 2007), quintic polynomial in PH form was considered in Habib and Sakai (2010). However, this method does not provide CCA with reference to curvatures at the endpoints of a segment.

1.3. Contributions

Our proposed method overcomes the above mentioned problems and provides CCA related to curvatures at the endpoints. We used a PH quintic function for the curvature continuous curve matching G^2 Hermite end conditions consisting of fixed endpoints, and tangents/curvatures at these endpoints. Curvature continuous conditions are derived on the whole segment and admissible area is visualized for a fair segment with reference to the curvatures at its endpoints under the given positional and tangential end conditions.

The rest of paper is structured as follows. Section 2 presents an overview of the notations and conventions that are used in subsequent sections along with theoretical background of PH quintic. Proposed methodology, curvature continuous conditions, and the derivation of admissible CCA are discussed in Section 3. Section 4 presents the algorithm that we developed based on our analysis in Section 3. This algorithm has been implemented and three numerical examples are given in Section 5 to illustrate. The relative merits of the proposed algorithm are briefly discussed in Section 6. Finally, paper is concluded in Section 7.

2. Preliminaries

Readers are referred to Habib and Sakai (2010, 2013) for conventions used in this paper and description of PH quintic Bézier function. The term 'CCA' relates to the admissible region in curvature space for a curvature continuous curve with respect to given positions at endpoints, tangents to the curve at endpoints, and curvatures at these endpoints.

We consider a PH quintic Bézier polynomial $\boldsymbol{z}(t) = (z_x(t), z_y(t))$ of Farin (2002), Habib and Sakai (2013) after transformation in normalized form

$$\boldsymbol{z}(t) = \sum_{i=0}^{5} \binom{5}{i} \boldsymbol{p}_i (1-t)^{5-i} t^i, \;\; 0 \leqslant t \leqslant 1, \tag{2.1}$$

which is plotted in Fig. 1. Farouki and Sakkalis (1990) considered the curve $\boldsymbol{z}(t)$ in PH quintic form $\boldsymbol{z}'(t) = (z_x'(t), z_y'(t))$ as

$$\boldsymbol{z}'(t) = (x(t), iy(t))^2 = (x^2(t) - y^2(t), 2x(t)y(t)), \quad 0 \leqslant t \leqslant 1, \tag{2.2}$$

where

$$x(t) = x_0(1-t)^2 + 2x_1 t(1-t) + x_2 t^2,$$
$$y(t) = y_0(1-t)^2 + 2y_1 t(1-t) + y_2 t^2, \tag{2.3}$$

simplifying the formula of curvature

$$\kappa(t) = \frac{2\{x(t)y'(t) - x'(t)y(t)\}}{\{x^2(t) + y^2(t)\}^2}, \tag{2.4}$$

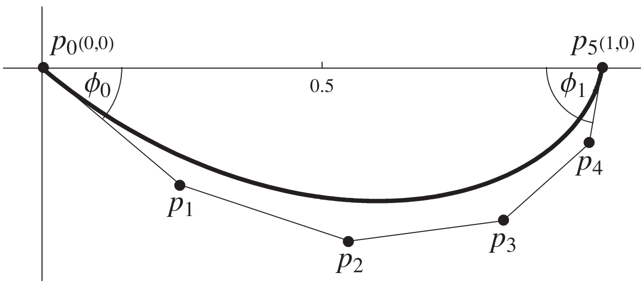

Fig. 1 A normalized PH quintic curve matching G^2 Hermite end conditions.

and its derivative $\kappa'(t)$ for later use (Habib and Sakai, 2013). Now Bézier control points in normalized form turn into Farouki and Neff (1995)

$$\begin{aligned}
\boldsymbol{p}_0 &= (0,0),\\
\boldsymbol{p}_1 &= \boldsymbol{p}_0 + \frac{1}{5}(x_0^2 - y_0^2, 2x_0y_0),\\
\boldsymbol{p}_2 &= \boldsymbol{p}_1 + \frac{1}{5}(x_0x_1 - y_0y_1, x_0y_1 + x_1y_0),\\
\boldsymbol{p}_3 &= \boldsymbol{p}_2 + \frac{1}{15}(2x_1^2 - 2y_1^2 + x_0x_2 - y_0y_2, 4x_1y_1 + x_0y_2 + x_2y_0),\\
\boldsymbol{p}_4 &= \boldsymbol{p}_3 + \frac{1}{5}(x_1x_2 - y_1y_2, x_1y_2 + x_2y_1),\\
\boldsymbol{p}_5 &= \boldsymbol{p}_4 + \frac{1}{5}(x_2^2 - y_2^2, 2x_2y_2)\ (= (1,0)).
\end{aligned} \tag{2.5}$$

To make sure the matching of G^2 Hermite end conditions, we assume the following without loss of generality.

1. the endpoints of quintic Bézier curve are $\boldsymbol{p}_0 = (0,0)$ and $\boldsymbol{p}_5 = (1,0)$.
2. the angle between the tangent to the curve at start point $\boldsymbol{p}_0$ and the vector $(1,0)$ is denoted by ϕ_0, while the angle between the vector $(1,0)$ and the tangent to the curve at endpoint $\boldsymbol{p}_5$ is denoted by ϕ_1.
3. the curvatures at start point $\boldsymbol{p}_0$ and endpoint $\boldsymbol{p}_5$ are κ_0 and κ_1, respectively.

3. G^2 Hermite curvature continuous curve

Curvature continuous fair curves are either of monotonically increasing or decreasing curvature. In this paper, we consider increasing curvature. Following conditions are required to guarantee the absence of any interior curvature extremum in quintic polynomial $\boldsymbol{z}(t)$ on parameter t, where $t \in [0,1]$:

1. $0 < \phi_0 < \phi_1 < \pi/2$.
2. The derivative of curvature $\kappa'(t)$ should not have root on $[0,1]$.

Next we derive a curvature continuous area under the fixed Hermite end conditions. First we consider given end tangent conditions, i.e., angle ϕ_0 from the tangent to the curve at its start point $\boldsymbol{z}(0)$ and angle ϕ_1 from the horizontal axis to the tangent to the curve at its endpoint $\boldsymbol{z}(1)$, we have

$$\frac{z_y'(0)}{z_x'(0)} = \tan\phi_0, \quad \frac{z_y'(1)}{z_x'(1)} = \tan\phi_1,$$

giving us

$$y_0 = -x_0\tan\frac{\phi_0}{2}, \quad y_2 = x_2\tan\frac{\phi_1}{2}, \tag{3.1}$$

for later use. Requirement of end point of curve, $\boldsymbol{p}_5 = (1,0)$, yields a system of equations in (x_1, y_1) as

$$\begin{aligned}
&2x_1^2 + 3(x_0+x_2)x_1 + (3x_0^2 + x_0x_2 + 3x_2^2)\\
&= 2y_1^2 + 3(y_0+y_2)y_1 + (3y_0^2 + y_0y_2 + 3y_2^2) + 15,\\
&6(x_0y_0 + x_2y_2) + 3x_1(y_0+y_2) + 4x_1y_1 + 3y_1(x_0+x_2)\\
&+ x_0y_2 + x_2y_0 = 0.
\end{aligned} \tag{3.2}$$

Here parameter x_0 is considered positive without any loss of generality. The following lemma is used to prove the Theorem 3.1.

Lemma 3.1. *Parameters $x_i, i = 0,1,2$ have the same sign if the angles from $\boldsymbol{p}_1\boldsymbol{p}_2$ to the horizonal axis and from the horizonal axis to $\boldsymbol{p}_3\boldsymbol{p}_4$ are $(0,\pi/2)$ (Habib and Sakai, 2010).*

Proof. Readers are referred to Habib and Sakai (2010) for the proof. □

For given curvatures κ_0 and κ_1 at the endpoints $t = 0$ and $t = 1$, respectively, of polynomial $\boldsymbol{z}(t)$ defined in (2.1), we have from (2.4) and (3.1) a set of two equations

$$\begin{aligned}
\kappa_0 &= \frac{4}{x_0^3}\left(x_1\tan\frac{\phi_0}{2} + y_1\right)\cos^4\frac{\phi_0}{2},\\
\kappa_1 &= \frac{4}{x_2^3}\left(x_1\tan\frac{\phi_1}{2} - y_1\right)\cos^4\frac{\phi_1}{2},
\end{aligned} \tag{3.3}$$

which can be solved for (x_1, y_1) as

$$\begin{aligned}
(x_1, y_1) = \frac{1}{4\sin\frac{\phi_0+\phi_1}{2}}\Bigg\{&\frac{\kappa_0 x_0^3}{\cos^3\frac{\phi_0}{2}}\left(\cos\frac{\phi_1}{2}, \sin\frac{\phi_1}{2}\right)\\
&+\frac{\kappa_1 x_2^3}{\cos^3\frac{\phi_1}{2}}\left(\cos\frac{\phi_0}{2}, -\sin\frac{\phi_0}{2}\right)\Bigg\}.
\end{aligned} \tag{3.4}$$

To simplify the further analysis, we assume

$$(x_0, x_2) = \sqrt{d}\left(\cos\frac{\phi_0}{2}, m\cos\frac{\phi_1}{2}\right), \tag{3.5}$$

and consider (x_1, y_1) above to reduce the system of equations in (3.2) to a quadratic and cubic equations in 'd', as shown in (3.6) and (3.7) below:

$$e_2d^2 + e_1d + e_0 = 0, \tag{3.6}$$

where

$$\begin{aligned}
e_2 &= \kappa_1^2m^6\sin\phi_0 + \kappa_0\left(2\kappa_1m^3\sin^2\frac{\phi_0-\phi_1}{2} - \kappa_0\sin\phi_1\right),\\
e_1 &= 6\sin\frac{\phi_0+\phi_1}{2}\left\{\kappa_1m^3\sin\phi_0 + (\kappa_0 + \kappa_1m^4)\sin\frac{\phi_0-\phi_1}{2} - \kappa_0m\sin\phi_1\right\},\\
e_0 &= 8\sin^2\frac{\phi_0+\phi_1}{2}\left\{3\sin\phi_0 + m\sin\frac{\phi_0-\phi_1}{2} - 3m\sin\phi_1\right\},
\end{aligned}$$

and,

$$f_3d^3 + f_2d^2 + f_1d + f_0 = 0, \tag{3.7}$$

where

$$f_3 = \kappa_1^2 m^6 \cos\phi_0 + \kappa_0\left(2\kappa_1 m^3 \cos\frac{\phi_0-\phi_1}{2} + \kappa_0\cos\phi_1\right),$$
$$f_2 = 6\left\{\left(\kappa_0+\kappa_1 m^4\right)\cos\frac{\phi_0-\phi_1}{2} + m\left(\kappa_1 m^2\cos\phi_0 \right.\right.$$
$$\left.\left. +\kappa_0\cos\phi_1\right)\sin\frac{\phi_0+\phi_1}{2}\right\},$$
$$f_1 = 8\left\{3\cos\phi_0 + m\left(\cos\frac{\phi_0-\phi_1}{2}+3m\cos\phi_1\right)\right\}\sin^2\frac{\phi_0+\phi_1}{2},$$
$$f_0 = 120\sin^2\frac{\phi_0+\phi_1}{2}.$$

To further simplify the analysis on derivative of curvature, we can transform the unit interval of parameter t from $[0,1]$ to $[0,\infty)$ by replacing t with $1/(1+s)$, introducing another parameter s having lower bound only. Therefore, the derivative of curvature $\kappa'(t)$ for $t = 1/(1+s)$, becomes

$$\|z'(t)\|^5\kappa'(t) = \frac{4}{(1+s)^5}\sum_{i=0}^{5} h_i s^i, \tag{3.8}$$

for

$$h_i = F_i[x_2,x_0,y_2,y_0], \quad i=0,1,2,$$
$$= F_{5-i}[x_0,x_2,y_0,y_2], \quad i=3,4,5,$$

in symmetric form, where

$$\begin{aligned}
F_0[p,q,r,s] &= (p^2+q^2)\{ps-qr+6(py_1-rx_1)\} - 8(p^2-r^2)x_1y_1 \\
&\quad + 8pr(x_1^2-y_1^2),\\
F_1[p,q,r,s] &= 7(p^2+r^2)(ps-qr) + 2(6pqr-p^2s+5r^2s)x_1\\
&\quad - 2(6prs-qr^2+5p^2q)y_1 + 16(p^2-q^2)x_1y_1\\
&\quad - 16pr(x_1^2-y_1^2) + 16(rx_1-py_1)(x_1^2+y_1^2),\\
F_2[p,q,r,s] &= 6qs(r^2-p^2) + 6pr(q^2-s^2) + 4(r^2s+7p^2s-6pqr)x_1\\
&\quad - 4(p^2q+7qr^2-6prs)y_1 - 24(pq-rs)x_1y_1\\
&\quad - 8(rx_1-py_1)(x_1^2+y_1^2)\\
&\quad + 12\{x_1^2(3qr-ps)+y_1^2(qr-3ps)\}.
\end{aligned} \tag{3.9}$$

We can analytically formulate the problem of generating PH quintic curvature continuous curve by finding conditions on the coefficients of the quintic polynomial in (3.8) to make sure it has non-positive roots.

3.1. Necessary and sufficient conditions for the curvature continuous curve

Since the osculating circle at the start point of curve $\boldsymbol{p}_0$ is completely inside the osculating circle at the endpoint of curve $\boldsymbol{p}_5$, we can find the necessary conditions for a curvature continuous curve, discussed in Dietz and Piper (2004), Dietz et al. (2008), Habib (2010), and are formulated as

$$\kappa_0 < 2\sin\phi_0, \quad \kappa_1 > \frac{2\{1-\cos(\phi_0+\phi_1)-\kappa_0\sin\phi_0\}}{2\sin\phi_0-\kappa_0}. \tag{3.10}$$

Above conditions provide boundaries of the area in which any curvature continuous curve may be achieved. These boundaries are highlighted by dark solid hyperbolas in Figs. (a)(a)2–4(a). Admissible curvature continuous area in a given curvature space within these boundaries is based on Theorem 3.1 and its numerical derivation is discussed in Section 3.2.

The following theorem gives us sufficient curvature continuous conditions on tangent angles (ϕ_0,ϕ_1) and curvatures (κ_0,κ_1) at the endpoints of the curve, where $0<\phi_0<\phi_1<\pi/2$ and $0<\kappa_0<\kappa_1$.

Theorem 3.1. *The Bézier curve of quintic order (2.1) in PH form is a monotonically increasing curvature continuous if h_i, $i=0,2,3,5$ are non-negative and*

$$h_1 \geqslant -2\sqrt{h_0h_2}, \quad h_4 \geqslant -2\sqrt{h_3h_5}. \tag{3.11}$$

Proof. Since curvature κ_0 at start point of the segment $\boldsymbol{z}(t)$ is positive in (3.3), first the condition

$$x_1\tan\frac{\phi_0}{2} + y_1 > 0, \tag{3.12}$$

is considered then Descartes rule of signs is applied due to the fact

$$a+bu+cu^2 \geqslant a+2\sqrt{ac}+cu^2 = \left(\sqrt{a}+\sqrt{c}u\right)^2,$$

the PH quintic Bézier curve (2.1) is a curvature continuous curve if conditions in (3.11) hold. □

3.2. Admissible CCA in curvature space

In this section we consider the problem of searching for an admissible area for a PH quintic curvature continuous curve with respect to the curvatures (κ_0,κ_1) at its endpoints under the fixed Hermite end conditions. For given (ϕ_0,ϕ_1), we numerically determine the admissible CCA in a curvature space of (κ_0,κ_1) within the range given in (3.10). First we solve analytically the quadratic Eq. (3.6) for the solution

$$(d_1,d_2) = \left(\frac{-e_1+\sqrt{e_1^2-4e_0e_2}}{2e_2}, \frac{-e_1-\sqrt{e_1^2-4e_0e_2}}{2e_2}\right), \tag{3.13}$$

and apply the Newton–Raphson method for the solution of (3.7) for m. If we find any (d,m) satisfying sufficient conditions in (3.11) then $(\phi_0,\phi_1;\kappa_0,\kappa_1)$ give a curvature continuous segment with fixed given endpoints.

4. The algorithm

An algorithm for finding curvature continuous PH quintic polynomial is given in this section for implementation of our proposed method in the previous section. As before, we have adopted the heuristic approach to construct a G^2 Hermite fair curve using a single polynomial in PH quintic Bézier form. The algorithm has the following steps.

1. Given are endpoints $\boldsymbol{A}$ and $\boldsymbol{B}$ of the required spiral segment, tangent angles at endpoints (ϕ_0,ϕ_1) and curvatures at endpoints (κ_0,κ_1), satisfying necessary conditions in (3.10).
2. Normalize the given data by transformation as per Fig. 1 such that endpoints $\boldsymbol{A}$ and $\boldsymbol{B}$ become $\boldsymbol{p}_0=(0,0)$ and $\boldsymbol{p}_5=(1,0)$, respectively.
3. Find (d,m) and the curvature continuous area for (ϕ_0,ϕ_1) as per procedure given in Section 3.2.
4. If (κ_0,κ_1) belongs to the curvature continuous area then go to the next step, otherwise fair curve does not exist for the given data.
5. Find (x_0,x_2), (y_0,y_2) and (x_1,y_1) from (3.5), (3.1) and (3.4), respectively.
6. Find middle control points $\boldsymbol{p}_i$, $i=1,2,\ldots,4$, from (2.5).
7. Obtain the desired fair curve from (2.1).

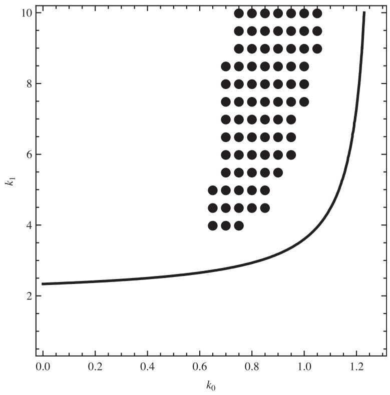

(a) Curvature continuous area for $(\phi_0, \phi_1) = (0.7, 1.4)$

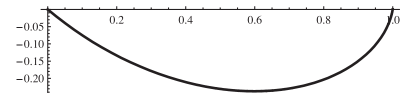

(b) Curvature continuous curve matching $(\phi_0, \phi_1) = (0.7, 1.4), (\kappa_0, \kappa_1) = (0.9, 5.5)$

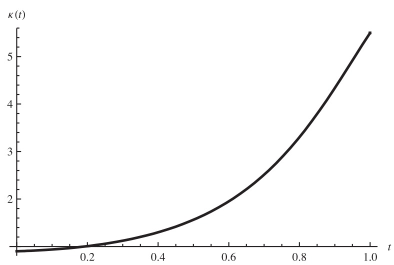

(c) Plot of $\kappa(t)$

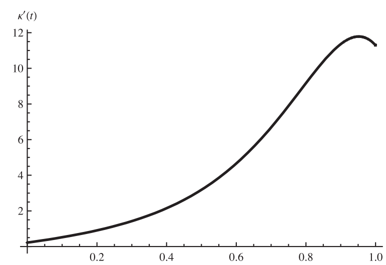

(d) Plot of $\kappa'(t)$

Fig. 2 Curvature continuous area with respect to curvatures at the endpoints and G^2 Hermite curvature continuous curves with their corresponding curvature and derivative of curvature plots.

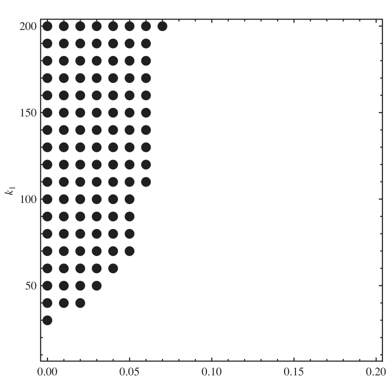

(a) Curvature continuous area for $(\phi_0, \phi_1) = (0.1, 1.5)$

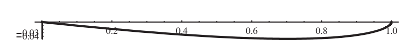

(b) Curvature continuous curve matching $(\phi_0, \phi_1) = (0.1, 1.5), (\kappa_0, \kappa_1) = (0.01, 200)$

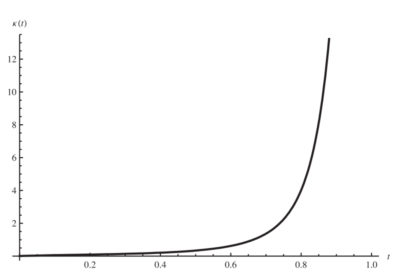

(c) Plot of $\kappa(t)$

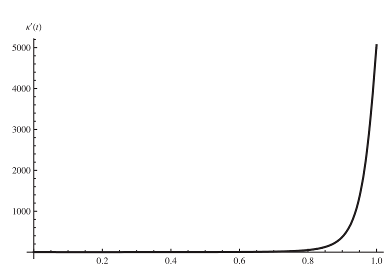

(d) Plot of $\kappa'(t)$

Fig. 3 Curvature continuous area with respect to curvatures at the endpoints and G^2 Hermite curvature continuous curves with their corresponding curvature and derivative of curvature plots.

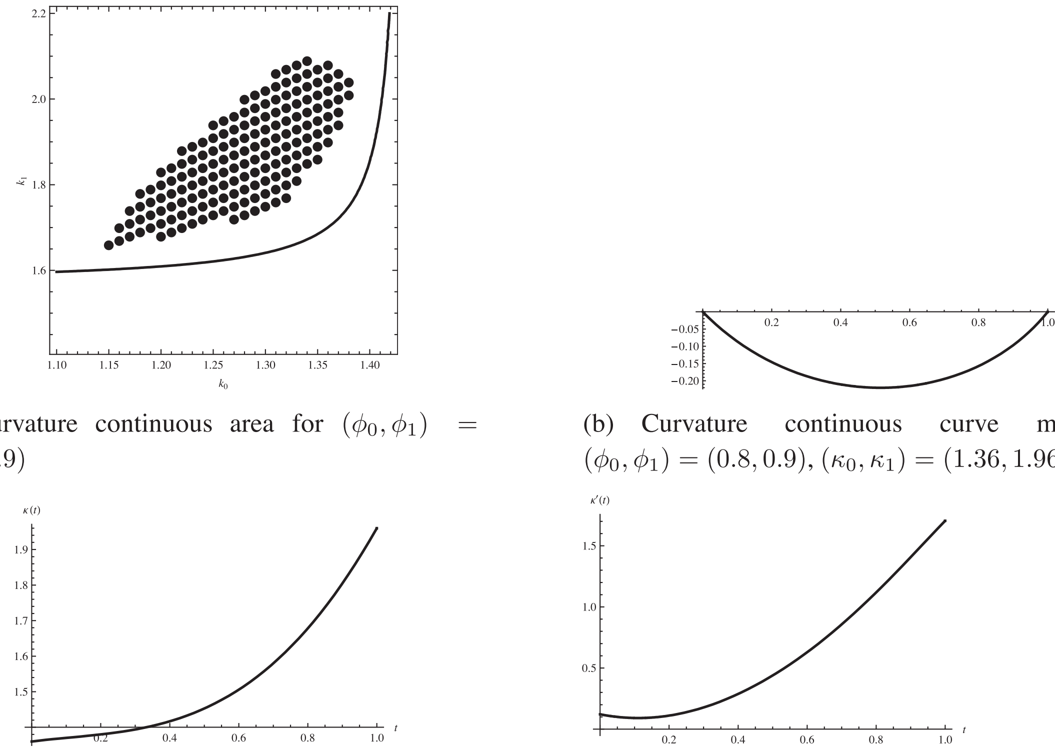

(a) Curvature continuous area for $(\phi_0, \phi_1) = (0.8, 0.9)$

(b) Curvature continuous curve matching $(\phi_0, \phi_1) = (0.8, 0.9)$, $(\kappa_0, \kappa_1) = (1.36, 1.96)$

(c) Plot of $\kappa(t)$

(d) Plot of $\kappa'(t)$

Fig. 4 Curvature continuous area with respect to curvatures at the endpoints and G^2 Hermite curvature continuous curves with their corresponding curvature and derivative of curvature plots.

8. Shift the transition curve back to its original location by applying inverse transformation.

5. Numerical examples

The above algorithm is used for the following three numerical examples of curvature continuous curves matching G^2 Hermite end conditions. All curvature continuous curves are plotted through the quintic polynomial in PH Bézier form. Our claim of curvature continuity is verified by curvature plots and derivative of curvature plots of all curves.

Example 1. First we consider a simple case. For tangent angles at endpoints $(\phi_0, \phi_1) = (0.7, 1.4)$, admissible curvature continuous area is shown as small disks in Fig. 2(a). Then curvature continuous segment for $(\kappa_0, \kappa_1) = (0.9, 5.5)$ is plotted in Fig. 2(b) with its corresponding curvature plot and derivative of the curvature plot in Fig. 2(c) and 2(d), respectively.

Example 2. Curvature continuous area for $(\phi_0, \phi_1) = (0.1, 1.5)$, with respect to curvatures at the endpoints is shown in Fig. 3(a). Then curvature continuous segment for $(\kappa_0, \kappa_1) = (0.01, 200)$ is plotted in Fig. 3(b) with its corresponding curvature plot and derivative of the curvature plot in Fig. 3(c) and 3(d), respectively. This example shows that our proposed method successfully handles difficult end conditions when the curvature at the endpoint is much larger than the curvature at the start point.

Example 3. Here is another possible difficult case when the curvature at the endpoint becomes slightly larger than the curvature at the start point. Curvature continuous area for $(\phi_0, \phi_1) = (0.8, 0.9)$ is shown in Fig. 4(a). Then curvature continuous segment for $(\kappa_0, \kappa_1) = (1.36, 1.96)$ is plotted in Fig. 4(b) with its corresponding curvature plot and derivative of the curvature plot in Fig. 4(c) and 4(d), respectively.

6. Relative merits of the proposed method

Our methodology and algorithm of derivation of CCA for the spiral segment matching G^2 Hermite conditions are significantly simplified and free from hidden curvature extrema due to (i) the evaluation of the derivative of the curvature for arbitrary values on the whole segment instead of discretization (Dietz et al., 2008), (ii) the use of PH quintic polynomial as compared to the use of rational cubic with additional parameters causing the methodology to be lengthy and the algorithm more complicated (Habib and Sakai, 2010), (iii) the visualization of CCA in curvature space which is not provided by Habib and Sakai (2010).

7. Conclusion and future direction

We used a single quintic function in PH Bézier form to derive admissible regions for a curvature continuous segment matching G^2 Hermite end conditions exactly (the fifth case). It is beneficial for designers and implementers to use a single polynomial as they have to deal with fewer entities. Our scheme provides stable results without any fear of the spiking phenomenon of the non-monotone curvature as highlighted in Dietz et al. (2008). Due to the use of Descartes rule of sign, curvature continuous conditions are computationally stable. Our proposed method and algorithm easily handle the difficult cases, when the curvature at the endpoint is extremely larger than the curvature at the start point, or when the curvature at the endpoint is very close to the curvature at the start point.

Future research work on the subject can be continued for the possibility of necessary conditions of CCA or more wider CCA for spiral segments by using any other method of spiral condition derivations.

Acknowledgment

The authors owe their gratitude to the three anonymous referees for their valuable comments which have helped to improve the presentation of this manuscript.

References

Ait-Haddou, R., 1995. Mathematical methods for curves and surfaces. In: G^2 Approximation of an Offset Curve by Tschirnhausen Quartics. Vanderbilt University Press, pp. 1–10.

Burchard, H., Ayers, J., Frey, W., Sapidis, N., 1993. Designing fair curves and surfaces. In: Approximation with Aesthetic Constraints.

Deng, C., Ma, W., 2012. Matching admissible G^2 Hermite data by a biarc-based subdivision scheme. Comput. Aided Geom. Des. 29, 363 378.

Dietz, D.A., Piper, B., 2004. Interpolation with cubic spirals. Comput. Aided Geom. Des. 21 (2), 165–180.

Dietz, D.A., Piper, B., Sebe, E., 2008. Rational cubic spirals. Comput. Aided Des. 40, 3–12.

Farin, G., 2002. Curves and Surfaces for CAGD: A Practical Guide, fifth ed. Morgan-Kaufmann.

Farouki, R., Neff, C., 1995. Hermite interpolation by Pythagorean-hodograph quintics. Math. Comput. 64, 1589–1609.

Farouki, R., Sakkalis, T., 1990. Pythagorean hodographs. IBM J. Res. Dev. 34 (5), 736–752.

Habib, Z., 2010. Spiral Function and Its Application in CAGD. VDM Verlag, Germany, ISBN 978-3-639-24988-0.

Habib, Z., Sakai, M., 2007a. G^2 Pythagorean hodograph quintic transition between two circles with shape control. Comput. Aided Geom. Des. 24 (5), 252–266.

Habib, Z., Sakai, M., 2007b. On PH quintic spirals joining two circles with one circle inside the other. Comput. Aided Des. 39 (2), 125–132.

Habib, Z., Sakai, M., 2008. Transition between concentric or tangent circles with a single segment of G^2 PH quintic curve. Comput. Aided Geom. Des. 25 (4–5), 247–257.

Habib, Z., Sakai, M., 2010. Admissible regions for rational cubic spirals matching G^2 Hermite data. Comput. Aided Des. 42 (12), 1117–1124.

Habib, Z., Sakai, M., 2010. Interpolation with PH quintic spirals. In: The Proceedings of IEEE International Conference on Computer Graphics. IEEE Computer Society Press, USA, pp. 80–85.

Habib, Z., Sakai, M., 2011. Cubic spiral transition matching G^2 Hermite end conditions. Numer. Math. Theory Methods Appl. 4 (4), 525–536.

Habib, Z., Sakai, M., 2012. Fairing arc spline and designing by using cubic Bézier spiral segments. Math. Model. Anal. 17 (2), 141–160.

Habib, Z., Sakai, M., 2013. Fairing an arc spline and designing with G^2 PH quintic spiral transitions. Int. J. Comput. Math. http://dx.doi.org/10.1080/00207160.2012.744452.

Hanmandlu, M., Shantaram, V., Krishna, V., 2003. Surface reconstruction from multiple views of painted curves. J. King Saud University – Comput. Inf. Sci. 15, 1–34.

Hartman, P., 1957. The highway spiral for combining curves of different radii. Trans. Am. Soc. Civil Eng. 122, 389–409.

Meek, D.S., Walton, D.J., 1989. The use of Cornu spirals in drawing planar curves of controlled curvature. Comput. Appl. Math. 25, 69–78.

Sarfraz, M. (Ed.), 2004. Geometric Modeling: Techniques, Applications, Systems and Tools. Kluwer, Netherlands.

Sarpono, D., Habib, Z., Sakai, M., 2009. Fair cubic transition between two circles with one circle inside or tangent to the other. Numer. Algorithms 51 (4), 461–476.

Walton, D.J., Meek, D.S., 2007. G^2 curve design with a pair of Pythagorean hodograph quintic spiral segments. Comput. Aided Geom. Des. 24 (5), 267–285.

Walton, D.J., Meek, D.S., Ali, J.M., 2003. Planar G^2 transition curves composed of cubic Bézier spiral segments. Comput. Appl. Math. 157 (2), 453–476.